4

Analysis of the reaction intermediates for propylene dehydrogenation on clean and sulphated Pt(111) surfaces

We have investigated the thermodynamics of the dehydrogenation of propylene to propylidyne on Pt(111) for a 0.25 ML coverage. We have determined the adsorption energies and most favourable adsorption sites for propylene, propylidyne and all the C_3H_x (x=3–7) intermediates (1-propyl, 2-propyl, propylidene, 1-propenyl, 2-propenyl, propenylidene and propynyl). All the surface species are more stable than gas phase propylene. Propylidyne is the most stable one in agreement with experiments. All of the surface moieties adsorb on sites where the number of metal atoms replace the missing hydrogen and preserve a sp^3 hybridisation. We used the adsorption energies to compute the overall reaction energies for a number of elementary C–H bond activation and isomerisation reactions that are likely to be involved in the dehydrogenation of propylene. The combination of energy and vibrational frequency calculations allowed us to propose some species as possible intermediates of the decomposition process.

We also studied the co-adsorption of propylene and sulphate species and the formation of an alkyl-sulphate intermediate. We proposed a structure for this intermediate and demonstrated the activation of the propylene molecule via its formation.

This chapter is organised as follows: section 4.1 is a brief review of the literature published on the adsorption of propylene and its subsequent decomposition to propylidyne on clean and sulphated Pt(111); section 4.2 discusses the adsorption and analyses the simulated vibrational spectra of propylene and the various C_3H_x dehydrogenation intermediates and compares the results obtained with the experimental data available; section 4.3 deals with the co-adsorption of propylene and sulphate and investigates the formation of alkyl-sulphate intermediates; section 4.4 recaptures the main conclusions from foregoing sections.

4.1 Introduction

Fundamental studies of alkene chemistry over catalytically active transition metal surfaces play a key role in efforts to understand and improve diverse catalytic processes ranking from pollution control to fine chemicals synthesis. Consequently, the chemisorption of olefins has extensively been investigated with a view to determining adsorption geometries and the nature and stability of reaction intermediates and products [1]. With this aim several experimental techniques have been developed. Infrared spectroscopy has widely demonstrated its ability to identify atoms and molecules at the metal surface and probe their immediate environment in 'real' reaction conditions. Despite the high performance of this technique, the low concentrations and short lifetimes of reaction intermediates make their identification quite challenging. The determination of vibrational frequencies by *ab initio* computational methods is becoming increasingly important in many areas of the chemistry. Such an area is the identification of reactive intermediates for which the theoretically predicted frequencies can serve as a fingerprint.

The interaction of ethylene (CH_2=CH_2) with Pt (111) has been extensively used as a model system to understand alkene hydrogenation-dehydrogenation processes. At low temperatures ethylene adsorbs on the Pt(111) surface in a di-σ mode forming a (2x2) pattern. Upon heating above 300 K it transforms into a new more stable species, ethylidyne [2,3,4], also with a (2x2) structure (after exposure to the electron beam of a LEED gun). This molecule is stable roughly between 300 and 420 K. The ethylene-to-ethylidyne transition represents the whole class of reactions, namely, the dehydrogenation of alkenes to alkylidynes. This reaction is believed to be involved in catalytic hydrogenation and dehydrogenation processes. In order to obtain ethylidyne, one H atom has to migrate from one C atom to the other and another one has to be abstracted from the molecule. Then, it is reasonable to assume that the mechanism consists of at least two steps and involves the formation of one or more intermediates. The details of this surface process have been source of an intense debate. Several simple mechanisms have been proposed with intermediates ethyl ($CH_3CH_2^*$), vinyl (CH_2CH^*), ethylidene (CH_3CH^*) and/or vinylidene (CH_2C^*) [5-11].

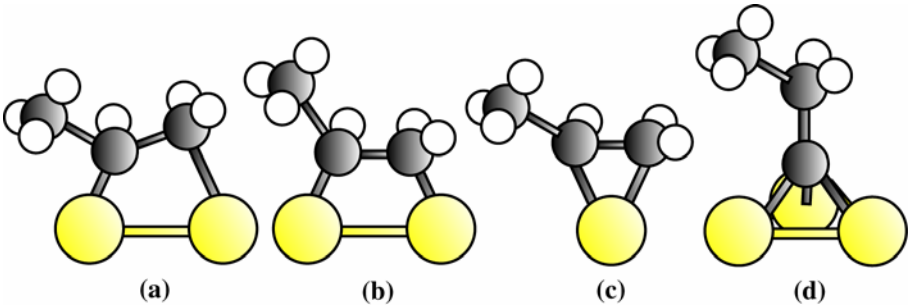

Scheme 4.1. Surface structures for the adsorption of propylene on Pt(111): propylene di-σ (V-shape) (a), propylene di-σ (b), propylene π (c), propylidyne (d).

The attempt to extend the preceding conclusions to all olefins has been unsuccessful because much less work has been carried out for bigger alkenes. Higher alkenes are also postulated to decompose via corresponding alkylidyne intermediates. After ethylene, propylene ($CH_3CH=CH_2$) is the most important raw material used in the production of organic chemicals. Early in 1982, Salmerón and Somorjai have shown that propylene adsorbs easily on the Pt(111) surface and remains stable without any chemical decomposition up to around 280 K [12]. Using Thermal Desorption Spectroscopy (TDS) these authors have estimated an adsorption energy of –51 $kJmol^{-1}$ at low coverages. Koestner *et al.* [4], using Low Energy Electron Diffraction (LEED), have proposed that propylene binds to two surface Pt atoms through its unsaturated C=C unit (di-σ-bond) and forms a disordered monolayer. Their results are in agreement with other experimental works [13,14] and with the results issued from qualitative molecular orbital calculations [15]. Besides, Koel and co-workers have also investigated the adsorption and decomposition of propylene on Pt(111) [16]. They have determined an adsorption energy of ~ –70 $kJmol^{-1}$. However, this rather simple picture of the interaction of propylene with Pt(111) contrasts with the complexity that emerges from the complete reflection-absorption (RAIRS) studies of Zaera *et al.* [17]. These authors have proposed that at least four species derive from adsorbed propylene as a function of coverage and the temperature (see **Scheme 4.1**). At T < 230 K this molecule adsorbs undissociated on Pt(111), in an analogous way to ethylene [18]. Below half-saturation, propylene binds to the metal surface in a di-σ fashion preferentially through its central C atom (V-shape). As the coverage increases up to saturation, the molecule rearranges. The C=C bond becomes more horizontal and the methyl group tilts towards a more vertical orientation. Comparison of infrared data from propylene ligands in osmium organometallic complexes to EELS and RAIRS data for propylene on Pt(111) and on Ni (111) [19] corroborates the di-σ-adsorption mode with a large degree of rehybridisation of the C towards sp^3 but does not provide further information on the structure of the adsorbed molecule. Above saturation coverage, a second layer of weakly adsorbed molecules grows (π-bonded). They have observed a clear transformation between about 230 and 270 K. Actually, the 275 K RAIRS spectrum is consistent with the formation of an alkylidyne moiety: propylidyne ($CH_3CH_2C^*$). Koestner *et al.* [4] have also detected the formation of this species. They have found that the LEED-

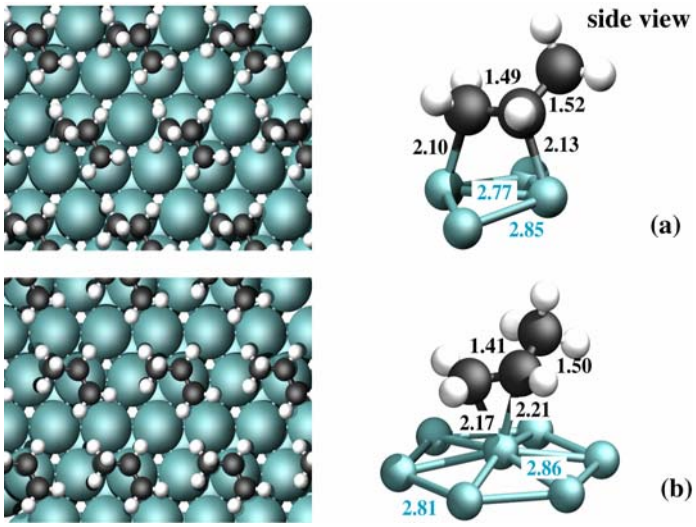

Figure 4.1. Stable adsorption modes for propylene on clean Pt(111) surface for a 2x2 unit cell: bridge (a) and top (b).

IV spectra of ethylene and propylene are roughly identical between 280 K and 400 K. This has been interpreted to imply that the room temperature propylene has a structure similar to room temperature ethylene. Data are consistent with the presence of an alkylidyne species. Contrasting with the non-spontaneous ordering of ethylidyne, propylidyne forms spontaneously a 2x2 pattern due to steric considerations. The formation of an intermediate during the transformation from propylene-to-propylidyne seems to be evident according to the new 2890 cm^{-1} feature observed in the 256 and 268 K RAIRS spectra. This signal cannot be associated with propylene nor propylidyne but may be matched with 2-propyl ($CH_3(CH_3)CH^*$) or propylidene ($CH_3CH_2CH^*$) species. Clearly, the accurate description of the structure of propylene and the possible reaction intermediates seems a necessary step towards understanding subsequent surface processes. No unequivocal determination of the mechanism has been accomplished. The best guess is the initial isomerisation of the adsorbed alkene to propylidene (1,2 hydrogen shift) and dehydrogenation to the alkylidyne moiety. Moreover, previous TDS experiments [20] have suggested that the propylene-to-propylidyne conversion may be accompanied by other decomposition reactions since more than one H atom per molecule are desorbed in the TDS spectra.

Especially interesting is the interaction of propylene with poison or promoter species present on the metal surfaces during the hydrogenation-dehydrogenation processes. Sulphoxy species are commonly occurring poisons during hydrocarbon combustion [21]. Exhaustive studies have investigated the influence of surface sulphoxy species in the hydrocarbon oxidation over platinum single-crystal surfaces and practical catalysts [22-26]. Lee *et al.* [25,26] have suggested that pre-adsorbed surface sulphate promotes room temperature propylene combustion associated with the decomposition of a thermally

Table 4.1. Computed adsorption energies ($kJmol^{-1}$) and geometries (distances in Å and angles in degrees) for propylene at a 1/4 and 1/9 ML coverage

Slab model	**bridge**		**top**	
Unit cell	**2x2**	**3x3**	**2x2**	**3x3**
E_{ads}	–87	–100	–51	–74
distance C^1–C^2	1.49	1.49	1.41	1.41
distance C^2–C^3	1.52	1.52	1.50	1.50
angle C^2–C^1H_2	129	131	153	153
distance C^1/C^2–Pt	2.10/2.13	2.11/2.14	2.17/2.21	2.20/2.22

unstable surface alkyl-sulphate complex. This complex decomposes to liberate CO_2 and SO_2. Nevertheless, the structure and properties of such adsorbed complex remain unknown. As on clean Pt(111), propylidyne is also formed.

Our main goal was to perform a systematic study of the adsorption structures and energetics of the propylene molecule and the possible intermediates of the dehydrogenation reaction. We used periodic DFT calculations to determine the geometry, adsorption site preference and adsorption energy for these species. We carried out a detailed analysis of vibrational spectra and focused our discussion on the comparison with experimental data. Finally, we explored the co-adsorption with sulphate to investigate possible formation of alkyl-sulphate intermediates during the dehydrogenation processes.

4.2 Clean Pt(111) surface

4.2.1 Adsorption of propylene

We explored several adsorption sites (top, bridge, hollow) for propylene on the clean Pt(111) surface. We found two stable surface structures. **Figure 4.1** shows these adsorption modes: bridge (**Figure 4.1a**) and top (**Figure 4.1b**). In both minima, the molecule binds to the metal surface through its C^1–C^2 bond, which sits almost parallel to the metal surface. The methyl group and hydrogen atoms are in some extend tilted away from the metal surface. In the bridge adsorption mode the C^1–C^2 bond axis is aligned along a Pt–Pt bond whereas in the top structure the C^1–C^2 midpoint is above a Pt surface atom. These surface structures are in good agreement with those predicted from experiments [12,13,14,17]. The bridge structure corresponds to the di-σ adsorption mode and the top to the weakly adsorbed π mode.

We present the computed adsorption energies (E_{ads}) for these adsorption modes at 1/4 ML coverage in **Table 4.1**. The bridge (di-σ) surface structure is the most stable one with an adsorption energy of –87 $kJmol^{-1}$. The adsorption on top (π) is relatively close in energy at 36 $kJmol^{-1}$. The computed adsorption energy for the di-σ or bridge mode is higher than the value estimated by TDS experiments (~ –50 $kJmol^{-1}$ and –70 $kJmol^{-1}$ from refs. [12] and [16], respectively). This is not surprising if we take into account the tendency of PW91 to overestimate adsorption energies [27]. Moreover, it is difficult to compare the calculated

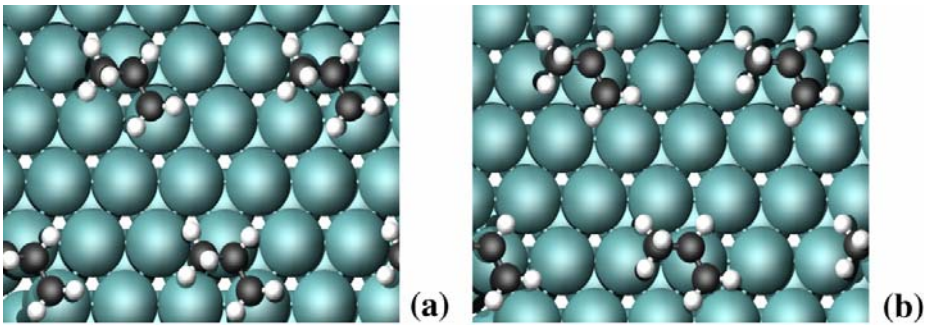

Figure 4.2. Stable adsorption modes for propylene on clean Pt(111) surface for a 3x3 unit cell: bridge (a) and top (b).

value with the experimental adsorption energy from TDS curves since propylene decomposition may occur before desorption takes place around 270–280 K [17]. Zaera and co-workers [17] proposed that at low coverages the hydrogen atom released in the dehydrogenation reaction (230–250 K) remains on the surface and weakens the adsorption of propylene. We computed the adsorption energy of the system propylene plus H atom at infinite distance (i.e. we calculated the E_{ads} of the hydrocarbon and the H separately. That is, the two fragments do not interact) and co-adsorbed on the same unit cell. Our calculations predict a decrease in the adsorption energy of 33 kJmol^{-1} on co-adsorption. Actually, the E_{ads} of the system molecule plus H atom at infinite distance is –144 kJmol^{-1} while for the co-adsorbed system is of –111 kJmol^{-1}.

We also investigated the coverage effects. We increased the size of the unit cell to 3x3, which corresponds to a molecular coverage of 1/9 ML (see **Table 4.1** and **Figure 4.2**). The adsorption energy increases from –87 kJmol^{-1} (2x2) to –100 kJmol^{-1}(3x3) and from –51 kJmol^{-1} (2x2) to –74 kJmol^{-1} (3x3), for the bridge and top structures, respectively. The energy difference (~ 13–23 kJmol^{-1}) is indicative of the existence of a slight repulsion between the propylene molecules at a 1/4 ML coverage. Despite the changes in E_{ads}, the bridge adsorption mode is still the more stable. Moreover, our results for the bridge adsorption site at a 1/9 ML coverage are in good agreement with the adsorption energy (–90 kJmol^{-1}) obtained by Delbecq and Sautet [28] using US-PP.

We summarise the distortion of propylene and the changes in the Pt–Pt bond distances upon adsorption in **Table 4.1** and **Figure 4.1** (side view). Gas phase propylene has a calculated C^1–C^2 bond distance of 1.33 Å and a C^2–C^1H_2 angle of 180º [29]. The bond of chemisorbed species to the surface metal atoms usually tends to decrease the internal bond strengths of the molecules, leading to longer internal bond distances. On adsorption, the C^1–C^2 distance increases significantly. Clearly, we found the most substantial increase for the bridge structure. The C^1–C^2 bond length is 1.49 Å. Interestingly enough, this bond distance is close to the obtained for di-σ adsorbed ethylene on Pt(111) using similar computational approaches [30,31]. This represents an elongation of 0.16 Å with respect to the free propylene, thus approaching a single C–C bond length as in propane (1.54 Å) with the concomitant reduction of the double bond character. Similar elongation has also been

Table 4.2. Computed adsorption energies ($kJmol^{-1}$) and geometries (distances in Å and angles in degrees) for propylene on a Pt_{33} cluster model

Cluster model	**bridge**		
Basis set[a]	3-21G/7Pt_l-26Pt_o	6-31G**/7Pt_l-26Pt_o	6-31G**/33Pt_l
E_{ads}	–49(9)	–23(8)	–61(–26)
distance C^1–C^2	1.49	1.50	1.50
distance C^2–C^3	1.53	1.52	1.52
angle C^2–C^1H_2	130	129	129
height C^1/C^2	2.11/2.16	2.07/2.12	2.07/2.12

[a]Basis set for adsorbate/substrate units. Results in parenthesis stand for the values corrected for the BSSE.

reported for different alkene molecules upon adsorption on Pt(111) [32,33]. For the top mode, the C^1–C^2 distance is 1.41 Å, which indicates that the sp^2 to sp^3 hybridisation is smaller. Another indicator of the degree of re-hybridisation of the C atoms is the C^2–C^1H_2 angle. Propylene loses its 'planarity' on adsorption as the CH bonds bend away from the surface plane. The angle between the H–C^1–H plane and the C^1–C^2 bond (parallel to the surface) for the bridge configuration (~ 130º) is larger than the angle for the top configuration (~ 153º). This fact confirms that the C atoms in the bridge structure have a higher degree of rehybridisation to sp^3.

For both minima, all the CH bond distances are 1.10 ± 0.01 Å. The rotation of the methyl group is almost free well in line with the results of propyne on different (111) metal surfaces (see **Chapter 3**).

As expected, the changes on the substrate are rather small. The relaxation of the surface metal atoms mainly involves an outwards movement of the Pt atoms directly bonded to the C ones. This produces a small corrugation of the surface (< 4%) with the simultaneous change of the Pt–Pt bond distances (< 0.16 Å).

We do not observe significant changes in the adsorption geometry when the coverage decreases (see **Table 4.1**).

Next we turn our attention to the description of the interaction of propylene on Pt(111) arising from the cluster model approach. We carried out these calculations using the Gaussian98 program [34] and the well-known hybrid B3LYP functional [35]. We represented the Pt(111) surface by a Pt_{33}(14,12,7) cluster model (the numbers in parenthesis indicate the number of atoms in each atomic layer) having Pt_7(4,3) as the *local* region and the remaining atoms defining the *outer* region [36]. The platinum atoms in the *local* region have been treated with the Hay-Wadt relativistic effective core potential [37] (RECP) which explicitly includes the $5s^25p^6$ semi-core electrons and the $5d^96s^1$ valence electrons and a (8s6p3d/3s3p2d) basis set. The remaining platinum atoms in the cluster have been treated with a one-electron RECP and a double-zeta basis set [38]. Let us recall that here the use of a cluster model is mainly aimed to investigate the limitations of the cluster model for the description of the propylene chemisorption. We corrected the adsorption energies for the Basis Set Superposition Error (BSSE), inherent to localised basis sets, using the standard Boys-Bernardi counterpoise method [39].

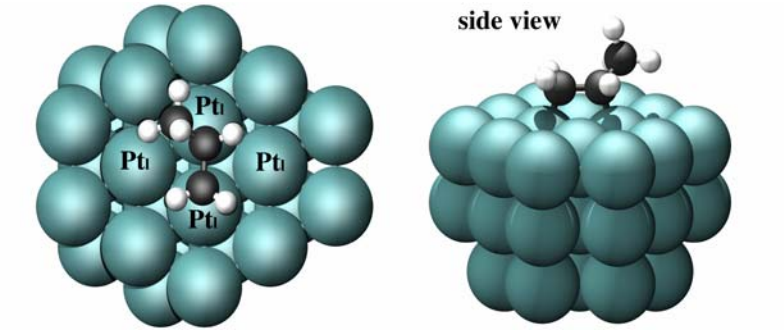

Figure 4.3. Adsorbed propylene on a Pt_{33} cluster model. Pt_l accounts for the Pt atoms in the *local* region.

We took the optimised geometry found in the slab calculations as starting point and re-optimised, maintaining the substrate frozen at the bulk geometry. Hence, the Pt-Pt distances were kept at the experimental bulk value of 2.77 Å [40]. In a preliminary set of calculations, we employed the 3-21G basis set for propylene. The calculated adsorption energy is –49 kJmol^{-1}. However, this value drops to 9 kJmol^{-1} once corrected for the BSSE (**Table 4.2**). To further improve the quality of this calculation, we re-optimised the structure with the more extended 6-31G** basis set for propylene. The adsorption energy decreases to –23 kJmol^{-1} but the BSSE corrected value of 8 kJmol^{-1} is still quite similar to the previous value. Finally, we improved the cluster model by treating all Pt atoms at the same level, i.e. explicitly including 18 electrons per Pt atom and the LANL2 basis set, using the geometry of the preceding point. The final BSSE corrected adsorption energy is –26 kJmol^{-1}. In all the cases, the adsorption geometry (**Figure 4.3** and **Table 4.2**) is in good agreement with the one obtained with the slab approach. Notice that the differences in C–C and C–Pt bond distances are rather small (<0.04 Å).

From this set of calculations, two important conclusions emerge. The most accurate cluster result for the adsorption energy is only ~ 30% of the one obtained in slab calculations. There are two reasons for this difference. First, a smaller value of the adsorption energy in the cluster model approach is not surprising; it arises from a too large Pauli repulsion between the cluster and the adsorbate. The overestimation of the Pauli repulsion comes from artificially confining the metal electron density in a reduced region, which reduces electron delocalisation. Second, the surface relaxation is not taken into account in the cluster calculations. Indeed, if one compares the cluster adsorption energy (–26 kJmol^{-1}) with the non-relaxed slab result (–39 kJmol^{-1}) the difference is reduced significantly.

Moreover, it is necessary a good description of the metal atoms (high quality basis set) with the concomitant increase of the computational cost.

Despite its good results for adsorption geometries, the poor description of adsorption energies and, more important, its high computational cost make cluster models not suitable to perform the study of the thermochemistry.

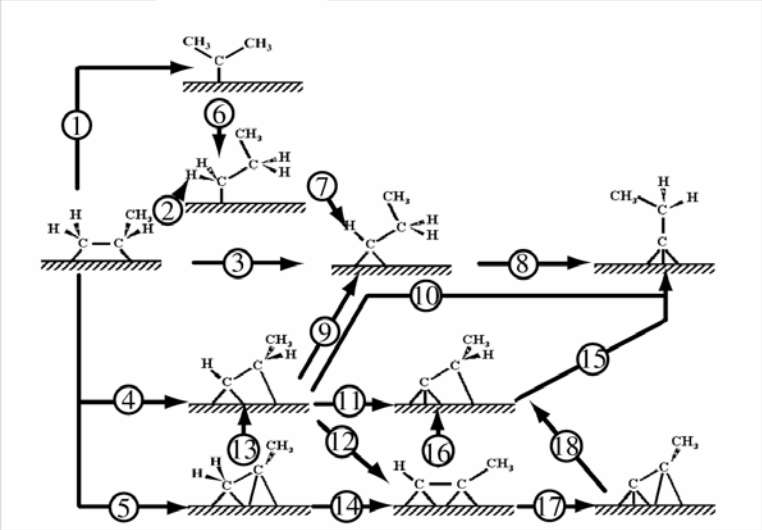

Scheme 4.2. Elementary paths for the decomposition of propylene to propylidyne on Pt(111).

4.2.2 Adsorption of C_3H_x (x=3–7) species

Scheme 4.2 shows the elementary paths for the dehydrogenation of di-σ bonded propylene to propylidyne. We did not consider the C–C bond breaking and we neglected the dehydrogenation of the methyl group. We determined the adsorption modes and the corresponding adsorption energies for all C_3H_x (x= 3–7) species using a 2x2 unit cell. The possible reaction intermediates are: 1-propyl ($CH_3CH_2CH_2^*$), 2-propyl ($CH_3(CH_3)CH^*$), propylidene ($CH_3CH_2CH^*$), propylidyne ($CH_3CH_2C^*$), 1-propenyl ($CH_3CH{=}CH^*$), 2-propenyl ($CH_3C^*{=}CH_2$), propyne ($CH_3C{\equiv}CH$), propenylidene ($CH_3CH{=}C^*$) and propynyl ($CH_3C{\equiv}C^*$). As for propylene, we explored different adsorption sites. Here, we show only the most stable identified configuration for each intermediate. The relative stabilities for each of the surface species are shown in **Figure 4.4**. We computed them with the formula

$$E_{ads} = (E_{C_3H_x/surface} - E_{surface} - E_{C_3H_{6(g)}}) - (x-6)(E_{H/surface} - E_{surface}) \qquad (4.1)$$

Equation (4.1) allowed us to obtain adsorption energies of the surface intermediates comparable with the adsorption energy of propylene. All the surface intermediates are more stable than the gas phase propylene. However, only four moieties are more stable than adsorbed propylene (1-propenyl, propylidyne, propenylidene and propyne, see **Figure 4.4**). Among them, the most stable one is the propylidyne species. Indeed, this species is –59 $kJmol^{-1}$ more stable than adsorbed propylene. In agreement with the experimental evidence [4,17,20], our calculations confirm that it is thermodynamically favourable for propylene to

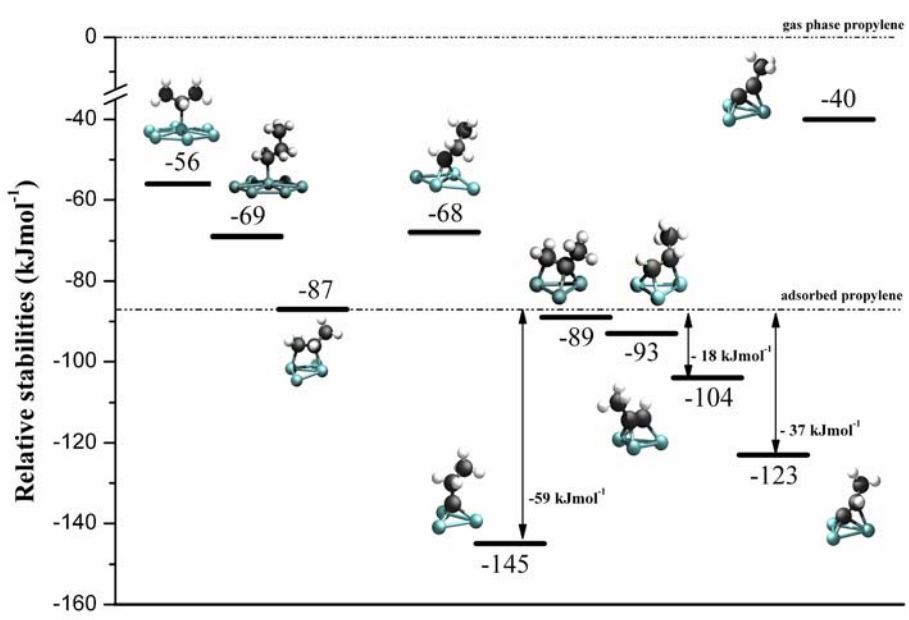

Figure 4.4 Energy profile for all the C_3H_x (x= 3–7) fragments on Pt(111) at1/4 ML coverage.

dehydrogenate to form propylidyne and surface hydrogen. 2-propenyl is almost isoenergetic with propylene (the energy difference is only 2 $kJmol^{-1}$). 1-propyl, 2-propyl, propylidene and propynyl are less stable by 18, 31, 19 and 47 $kJmol^{-1}$, respectively.

The calculated optimised structural parameters are illustrated in **Figures 4.5a-h**. For sake of clarity, we only represented the Pt atoms directly below the hydrocarbon fragment. Here, we do not present the adsorption geometry of propyne on Pt(111) because we have discussed it in the previous chapter (**§ 3, section 3.3.1**). 1-propyl (**Figure 4.5a**) and 2-propyl (**Figure 4.5b**) prefer the top adsorption site where the surface metal atom essentially replaces the missing hydrogen atom in order to form a 'propane-like' surface intermediate which preserves its sp^3 symmetry. This is consistent with concepts derived from Hoffmann [41] and Schustorovich and Baetzold [42] orbital interaction scheme. The balance between the Pauli repulsion and the orbital overlap dictates the adsorption site preference. For metals that lie to the right in the periodic table, Pauli repulsion dominates [43] and favours the top adsorption site for alkyl groups. Neurock and van Santen [44] have yet utilised these arguments to explain the adsorption site preference of ethyl groups on Pd(111). Propylidene (**Figure 4.5c**) is missing two hydrogen atoms in C^1 and therefore favours adsorption at a bridge site or η^2 (C^1)-adsorption mode (here, η^2 denotes the number of Pt atoms bind to a C atom). The C_3H_5 intermediates adsorb preferentially on hollow fcc sites. Propylidyne (**Figure 4.5d**) is missing three hydrogen atoms in C^1 and prefers to bind to three Pt atoms (η^3 (C^1) fashion). Our results are in good agreement with the experimental results of

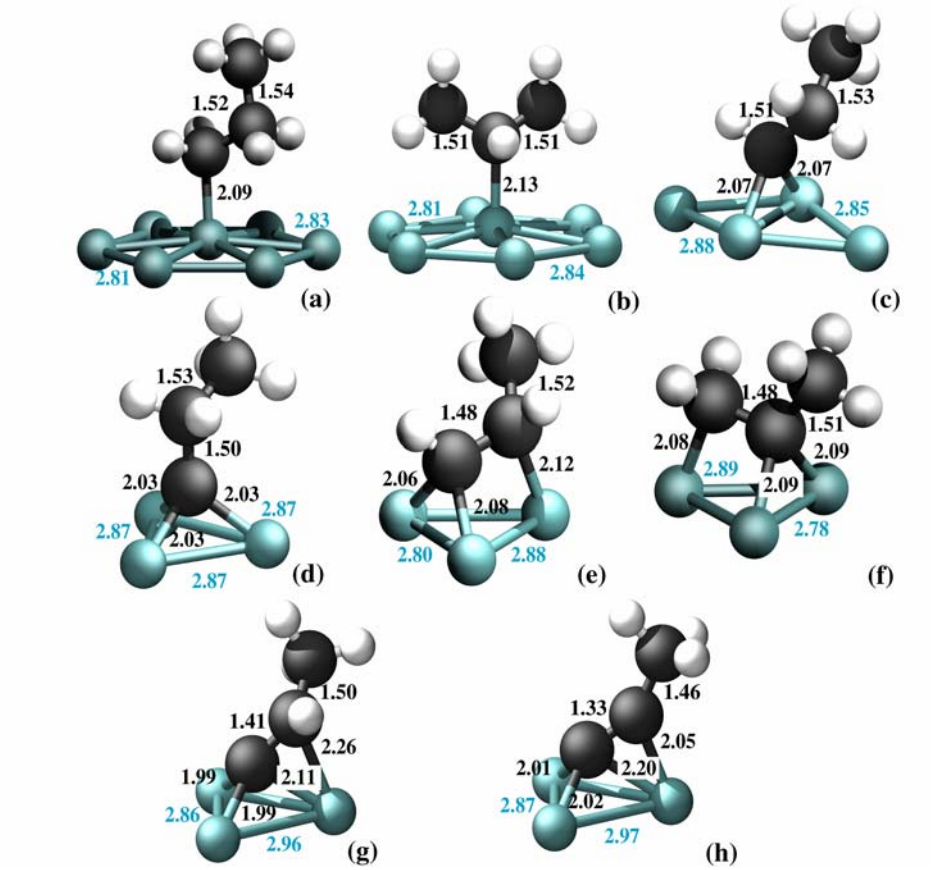

Figure 4.5. Adsorption geometries for the C_3H_x (x= 3-7) fragments on Pt(111) at 1/4 ML coverage. (a) 1-propyl, (b) 2-propyl, (c) propylidene, (d) propylidyne, (e) 1-propenyl, (f) 2-propenyl, (g) propenylidene and (h) propynyl. Distances in Å. Only the atoms directly below the hydrocarbon moiety are shown here for sake of visual clarity.

Koestner *et al.* [4]. These authors have determined that the propylidyne species is most likely adsorbed in the fcc hollow site on Pt(111). The 1-propenyl moiety (**Figure 4.5e**) is missing two H atoms in C^1 and one in C^2 and, therefore, it prefers the $\eta^2\eta^1(C^1,C^2)$-adsorption mode. The adsorption geometry of 2-propenyl (**Figure 4.5f**) is equivalent to the one obtained for 1-propenyl. There appears to be a general trend that Pt(111) prefers sp^3 bound intermediates. Actually, all the C–C bond distances are within the range 1.48-1.54 Å.

The picture for propenylidene (**Figure 4.5g**) and propynyl (**Figure 4.5h**) is quite different. Similarly to the C_3H_5 species, both surface intermediates adsorb preferentially on a 3-fold hollow site (fcc). The propenylidene moiety is missing three H atoms from C^1 and

Table 4.3. Calculated surface reaction energies (E_{reac}, $kJmol^{-1}$) for the decomposition of propylene on Pt(111)

step	Surface reaction	reaction	E_{reac}
1	propylene +H → 2-propyl	hydrogenation	31
2	propylene +H → 1-propyl	hydrogenation	18
3	propylene → propylidene	isomerisation	18
4	propylene → 1-propenyl +H	dehydrogenation	–6
5	propylene → 2-propenyl +H	dehydrogenation	–2
6	2-propyl → 1-propyl	isomerisation	–13
7	1-propyl → propylidene +H	dehydrogenation	1
8	propylidene → propylidyne +H	dehydrogenation	–77
9	1-propenyl +H → propylidene	hydrogenation	25
10	1-propenyl → propylidyne	isomerisation	–52
11	1-propenyl → propenylidene +H	dehydrogenation	–30
12	1-propenyl → propyne +H	dehydrogenation	–11
13	2-propenyl → 1-propenyl	isomerisation	–4
14	2-propenyl → propyne +H	dehydrogenation	–16
15	propenylidene +H → propylidyne	hydrogenation	–22
16	propyne → propenylidene	isomerisation	–19
17	propyne → propynyl +H	dehydrogenation	64
18	propynyl +H → propenylidene	hydrogenation	–83

one from C^2 and, therefore, it prefers to sit on $\eta^3\eta^1$ (C^1,C^2) fashion. However, the C^1–C^2 bond distance (1.41 Å) is rather short compared to the C_3H_x (x=5–7) hydrocarbon fragments (see above). Dumesic and co-workers have obtained the same adsorption site and geometry for vinylidene (CH_2=C^*) on Pt(111) [45]. However, propynyl binds clearly in a sp^2 fashion. This molecule is missing three H atoms from C^1 and two from C^2 to form a surface intermediate of sp^3 symmetry. However, it binds to the Pt(111) surface in a $\eta^3\eta^1$ (C^1,C^2) adsorption mode. C^2 only forms a bond with a metal atom. Moreover, the C^1–C^2 distance (1.31 Å) is obviously closer to a double bond (1.33 Å, propylene) than to a simple one (1.54 Å, propane).

Table 4.3 summarises the reaction energies for the various elementary steps depicted in **Scheme 4.2**. We computed the reaction energy (E_{reac}) by subtracting the energies of initial from the final state. For example, we calculated the energy for the propylene dehydrogenation to propylidyne by subtracting the energy of the adsorbed propylidene from the energy of the system propylidyne plus H adsorbed. In all the hydrogenation/dehydrogenation reactions, we assumed that the hydrocarbon moiety and the H atom do not interact.

Most of the steps listed in **Table 4.3** are either slightly endothermic or exothermic and would therefore still be possible in the mechanism of propylene decomposition. The formation of the propylidyne intermediate is always exothermic. This reaction can take place via dehydrogenation (8), isomerisation (10) or hydrogenation (15). The most favourable way to obtain this species is from propylidene (–77 $kJmol^{-1}$). Moreover, the surface reaction energetics suggests that the formation of propynyl is unlikely at this

Table 4.4. Calculated frequencies (in cm^{-1}) and intensities ($kmmol^{-1}$) for propylene on Pt(111)

experimental assignment	RAIRS[a] ν_i	2x2[b] ω_i	I_i	3x3[b] ω_i	I_i	theoretical assignment
CH_2 as st	2915(s)	3013	2.2	3053/3009	0.2/1.6	CH_3 as st
CH st	2883(s)	2986	0.1	2995	1.0	CH st
CH_3 s st+2xCH_3 as df	2860(m)	2933	9.9	2933	8.7	CH_3 s st
CH_2 s st	2830(w)	2982	2.0	2987	1.3	CH_2 s st
-	-	1434/1421	0.4/0.2	1434/1423	2.4/0.1	CH_3 as df
CH_2 sci	1437(m)	1400	0.1	1401	0.4	CH_2 sci
CH_3 s df	1375(w)	1337	0.1	1347	0.2	CH_3 s df
CH b	1309(w)	1296	0.3	1301	1.0	CH b
CH_2 wag	1260(w)	1161	0.2	1158	0.3	CH_2 twi
C^2–C^3 st	1088(s)	1092	0.9	1092	0.8	C^1–C^2 st/ C^2–C^3 st
CH_2 twi	1037(s)	1030	1.4	1033	1.9	CH_2 wag
CH_3 ro	1015(s)	1007	2.9	1008	7.5	CH_3 ro

key: as, asymmetric; s, symmetric; st, stretching; df, deformation; sci, scissoring; twi, twisting; wag, wagging; ro, rocking; b, bending; s, strong; m, medium; w, weak.
[a]values from ref 17; [b] this work.

coverage. The formation of this species by dehydrogenation of propyne is 64 uphill by $kJmol^{-1}$. Besides, its hydrogenation to propenylidene is highly exothermic (–84 $kJmol^{-1}$). Therefore, we suspect that propynyl is unlikely to be involved in the direct decomposition of propylene to propylidyne.

4.2.3 Analysis of vibrational spectra

To shed light on the nature of the surface intermediate of the propylene dehydrogenation to propylidyne, we computed the RAIRS spectrum for propylene (**Table 4.4**), propylidyne (**Table 4.5**) and all the possible reaction intermediates (1-propyl, 2-propyl, propylidene, 1-propenyl, 2-propenyl, propenylidene and propynyl, see **Appendix A.3**) on Pt(111) at 1/4 ML coverage. We analysed the spectrum of propyne on Pt(111) in **Chapter 3** (**section 3.3.3**).

Table 4.4 shows the frequencies along with the intensities for the di-σ propylene on Pt(111). We also computed the spectrum at 1/9 ML coverage (3x3 unit cell). The differences between these two models are not significant. Only the intensity of the bands at ~ 1430 and ~ 1000 cm^{-1} increases as the coverage decreases. We found that almost all the normal modes are coupled. This makes the description of the vibrations somewhat arduous and, in some cases, the assignment may be ambiguous. Our objective is not to analyse in detail the normal modes but to establish the differences among the surface species spectra that can help us to identify the possible reaction intermediates. Thus, the theoretical assignment accounts for the main vibrations for each feature. The experimental spectrum [17] presents four bands in the C–H stretching region (two of them quite intense); four medium or weak peaks in the 1500–1200 cm^{-1} range and three intense features in the 1000–1100 cm^{-1} region. Despite some differences in intensities and band assignment, our results

Table 4.5. Calculated frequencies (in cm^{-1}) and intensities ($kmmol^{-1}$) for propylidyne on Pt(111)

experimental assignment	RAIRS[a] ν_i	EELS[b] ν_i	RAIRS[c] ν_i	2x2[d] ω_i	I_i	theoretical assignment
CH_3 as st	2960(s)	2980(m)	2961(vs)	3044	5.2	CH_3 as st
CH_3 s st	2917(s)	2920(m)	2921(w)/2865(mw)	2970	4.4	CH_3 s st
2xCH_3 as df	2860(m)	-	-	-	-	-
CH_3 as df	1450(m)	1465(s)	1450(s)	1454	1.0	CH_3 as df
CH_2 sci	1408(m)	-	1407(m)	1399	0.4	CH_2 sci
CH_3 s df	1374(w)	-	-	1349	0.0	CH_3 s df
CH_2 wag	-	1295(w)	1303(w)	1265	0.1	CH_2 wag
C–C st	1104(m)	1115(s)	1103(s)	1087	4.1	C^1–C^2 st
CH_3 ro	1079(w)	1055(s)	1055(w)	1033	0.2	CH_3 ro
CH_3 ro	1041(m)	-	1039(s)	1026	0.0	CH_3 twi
C–C st	-	920(s)	929(s)	921	1.4	C^2–C^3 st

key: as, asymmetric; s, symmetric; st, stretching; df, deformation; sci, scissoring; twi, twisting; wag, wagging; ro, rocking; b, bending; s, strong; m, medium; w, weak.
[a]from ref 17; [b] from ref 13; [c]from ref 47; [d]this work.

are quite consistent with the experimental observations. The differences in the 2800–3100 cm^{-1} region arise from the poor description of the CH stretching modes [46]. Besides, both the experimental coverage and the experimental periodicity are not well reproduced. The arrangement of the molecules on the surface changes the orientation of the methyl groups and its environment. Zaera and co-workers [17] have pointed out that these changes strongly influence the band intensities.

Table 4.5 presents the calculated frequencies and intensities for propylidyne on Pt(111). For sake of comparison, **Table 4.5** also summarises the corresponding features in the RAIR [17,47] and EEL spectra [13] of propylene at ~ 300 K and saturation coverage. By analogy with the ethylene case, these studies have determined that these spectra arise from the propylidyne species. Our results fully confirm the experimental assignment (see **Table 4.5**). The agreement between the experimental and simulated spectra is fairly good. The main difference appears in the region around 900–1100 cm^{-1}. We assign the features at 1033, 1026 and 921 cm^{-1} to the CH_3 ro, CH_3 twi and the C^2–C^3 st, respectively. Only the peaks at 1033 and 920 cm^{-1} are intense. In the experimental RAIR spectrum, three intense peaks appear in this region. The bands at 1079[17]/1055[47], 1041[17]/1039[47] and 920 [47] cm^{-1} have been assigned to the CH_3 ro, CH_3 ro and C–C st, respectively. These differences may arise from the orientation of the neighbouring methyl groups. In our calculation all the methyl groups are oriented in the same direction. However, Koestner *et al*. [4] have suggested that the methyl groups tend to minimise the steric repulsions and, therefore, there are some orientations sterically not possible. Obviously, the one reproduced with the 2x2 unit cell is not the most favoured one.

The spectroscopic information available for the possible intermediates of the propylene-to-propylidyne transformation is scarce. Zaera *et al.* [17] have investigated the changes in the RAIR spectrum of propylene on Pt(111) as a function of the temperature

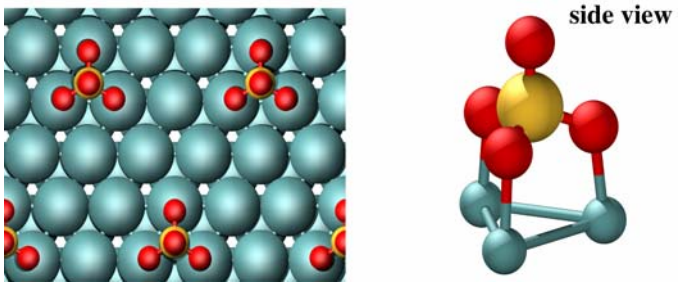

Figure 4.6. Sulphate on Pt(111) for a 3x3 unit cell.

(230–300 K). The formation of an intermediate seems to be evident. They have found that the spectrum at ~ 260 K includes a new signal at 2890 cm^{-1}. Moreover, this spectrum has no new peaks in deformation IR region. Actually, in the 1000–1500 cm^{-1} range, all the bands can be assigned to either propylene or propylidyne. They have proposed that these features may belong to the 2-propyl or to the propylidene species. We simulated and analysed the RAIRS spectra for all the proposed surface intermediates (see **Appendix A.3**). Unfortunately, the CH stretching region (2800–3100 cm^{-1}) is not well described with the harmonic model. Moreover, all the features lie in a small range and the differences are not big enough to be conclusive. We focused our attention in the deformation region (more specifically, on the features that can help us to rule out some species). The 1-propyl species has two signals at 1125 and 1350 cm^{-1} that are not visible either in the propylene spectrum or in the one of propylidyne. The features can be assigned to the CH_3 s df and to the CH_2 wag, respectively. 2-propyl has a quite strong feature at 1162 cm^{-1} (CH b mixed with the CH_3 ro). The propyne molecule, the 2-propenyl and the propenylidene moieties have some important peaks around 1350 cm^{-1} that are associated to the CH_3 s df. The propynyl intermediate has a strong feature at 1599 cm^{-1}, which can be assigned to the C=C st. However, the spectrum may be matched with those from propylidene or from 1-propenyl because these species have no important signals in the 1100–1400 cm^{-1} region. Unluckily, it is not possible to unequivocally identify the intermediate.

4.3 Sulphated Pt(111) surface

We investigated the formation of an alkyl-sulphate complex on co-adsorption of propylene and SO_4 on Pt(111) using a 3x3 unit cell (1/9 ML coverage). In the first place, we considered the adsorption of SO_4 on Pt(111). After a systematic exploration of the different adsorption modes (top, bridge, hollow), we conclude that SO_4 adsorbs on a three-fold hollow site, with a C_{3v} local symmetry. The three equivalent oxygen atoms are directly bound to three neighbouring Pt atoms while the fourth oxygen points upward (see **Figure 4.6**). All the Pt–O bond lengths are 2.11 Å; the internal S–O distances are 1.54 Å and 1.43 Å for the three equivalent oxygen atoms and the apical oxygen atom, respectively. The O–

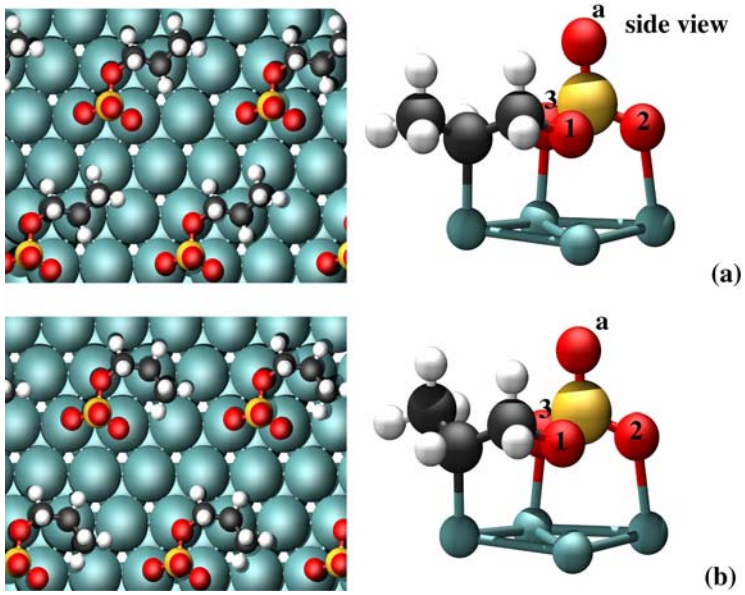

Figure 4.7. Alkyl-sulphate complex adsorbed on Pt(111) for a 3x3 unit cell: *trans* (a) and *cis* (b).

S–O angle involving two oxygen atoms directly bonded to the metal surface is 108º while the one related to the non-surface oxygen atom is 110º. The present results fully agree with those recently reported by Lin et al. [48] in their systematic theoretical study of sulphur oxides on Pt(111). Lee et al. [24,25] obtained surface sulphate adsorbing SO_2 onto oxygen pre-saturated Pt(111). Thus, we calculated the adsorption energy for SO_4 on Pt (111) with respect to the 2O/Pt(111) system (two adsorbed oxygen atoms per Pt unit cell) and the SO_2 molecule in gas phase. Following this procedure we obtained an adsorption energy of –127 $kJmol^{-1}$. If the reference is $SO_2 + O_2$ in the gas phase, the adsorption energy is –352 $kJmol^{-1}$, which is close to the value of –342 $kJmol^{-1}$ reported by Lin et al. [48] at the same coverage.

On co-adsorption with the propylene molecule a new alkyl-sulphate species may form. We found two different 'conformations' for this intermediate (see **Figure 4.7**). For sake of simplicity we named these structures *cis* (the methyl group and the sulphate lie in the same side of the C^1–C^2 bond) and *trans* (the SO_4 and the methyl group are in the opposite side of the C^1–C^2 bond). The energy difference between these two adsorption modes is quite small. Indeed, the *trans* surface structure is only 11 $kJmol^{-1}$ more stable than the *cis* adsorption mode. Experimentally propylene is adsorbed on sulphate pre-covered Pt(111) surface [25,26]. The energy gain due to the formation of this complex with respect to the sulphated surface and the free propylene is -70 $kJmol^{-1}$. Besides, the alkyl-sulphate complex and the co-adsorbed system (propylene and SO_4 adsorbed in the same unit cell) have the same relative stability. These results indicate that the formation of such a complex is quite

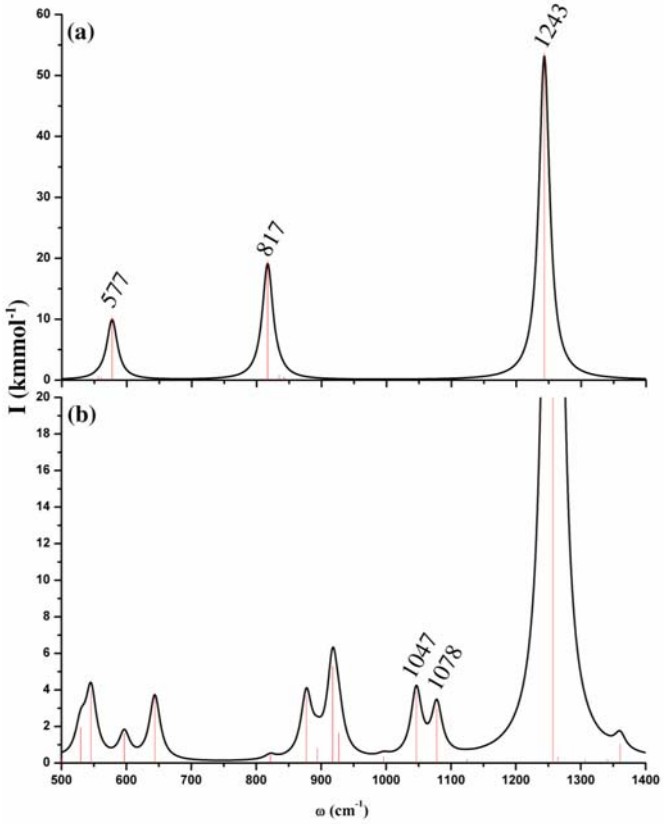

Figure 4.8. Simulated IR spectra for sulphate (a) and the alkyl-sulphate complex on Pt(111) for a 3x3 unit cell.

favourable on the Pt(111) surface.

The formation of the alkyl-sulphate complex changes significantly the surface geometry of both sulphate and propylene (see **Figure 4.7**). The SO_4 molecule binds to the C^1 of the hydrocarbon through one of its 'surface' oxygen atoms O^1. Hence, the additional C–O bond (1.47 Å) created may be the 'fingerprint' of this new species. As a consequence of the interaction, the sulphate moiety loses its C_{3v} symmetry. In the new structure only two oxygen atoms (O^2 and O^3) remain bound to the surface (see **Figure 4.7, side view**). Note that the oxygen atom that directly interacts with the propylene fragment (O^1) moves up to 2.51 Å. Moreover, we observe an important elongation of the two remaining Pt–O distances. On the SO_4/Pt(111) system, the Pt–O^2 and Pt–O^3 are equivalent. On co-adsorption, they increase to 2.31 Å (Pt–O^2) and 2.21 Å (Pt–O^3). The different Pt–O bond distances results from a small rotation of the sulphate fragment (~5º). Only the S-O^1

changes significantly (1.65 Å). The internal O-S-O angles vary as well: 112º (O_2–S–O_3), 105º (O^1–S–O^3) and 101º (O^1–S–O^2). The angles related to the apical oxygen atom are now 115º (O^2–S–O^a), 112º(O^3–S–O^a) and 108º (O^1–S–O^a).

The changes in geometry of the propylene molecule are more important than those observed for the sulphate species. The molecule is now adsorbed in a V-shape through its central C^2 atom. The C^1–C^2 bond length is 1.53 Å. This value is far away from those of gas-phase propylene (1.33 Å) and propylene on Pt (1.49 Å). Moreover, the H–C^1–H angle (109º). Clearly, the formation of this new species activates the propylene molecule.

Figure 4.8a-c illustrates the calculated vibrational spectra for the sulphate molecule (**Figure 4.8a**), and the alkyl-sulphate complex (**Figure 4.8b**) on Pt(111). Three peaks at 1243, 817 and 577 cm^{-1} dominate the spectrum of the SO_4 molecule. Our results are in good agreement with the experimental HREELS spectrum of SO_2 on oxygen-precovered Pt(111) [49] and previous DFT calculations of SO_4 on Pt(111) [48]. We assign the peak at 1243 cm^{-1} to the S-O^a stretching. The feature at 817 cm^{-1} corresponds to the SO_3 symmetric stretching of the three equivalent oxygen atoms vibrating in phase. Finally, we assign the band at 577 cm^{-1} to the SO_3 symmetric deformation of the oxygen atoms directly interacting with the metal surface. All these features also appear in the spectrum of the alkyl-sulphate complex (**Figure 4.8b**). We do not observed significant changes in the peak at 1243 cm^{-1}, well in line with the absence of major geometrical changes in the S-$O^{(a)}$ bond upon formation of the complex. However, the 817 and 577 cm^{-1} signals split because the three O atoms are not equivalent any more. Several weak features appear around 900 and 600 cm^{-1}. These bands correspond to the SO_3 stretch and the SO_3 deformation modes mixed with different modes of the hydrocarbon molecule. The two features at 1078 and 1047 cm^{-1} have some contribution of the new C–O bond formed (especially the 1047 cm^{-1} feature). Actually, these peaks are the 'fingerprint' of the alkyl-sulphate complex, since they appear in a region where there is no signal in the SO_4/Pt(111) spectrum and the peaks in the adsorbed propylene spectrum are very weak (see **section 4.2.3**). Values between 1000 and 1200 cm^{-1} are common in species where the oxygen atom is single-bonded to a sulphur atom. We computed the vibrational frequencies for dimethylsulphate in gas phase using the Gaussian98 code [34]. Indeed, for this molecule the C–O stretching appears at 1023 cm^{-1}.

4.4 Conclusions

We investigated the adsorption of propylene on Pt(111) by DFT. We found two stable surface structures: bridge (di-σ) and top (π). Our calculations indicate that the di-σ-bounded propylene is more stable than the π species. Actually, the computed adsorption energy for the di-σ-adsorption mode is –87 $kJmol^{-1}$ while that for the π mode is –51 $kJmol^{-1}$. The study of the coverage effects showed that the adsorption energy increases with decreasing the coverage (1/4 → 1/9 ML), but that the energy difference between the bridge and top structures remains roughly the same, with the former still more stable.

Moreover, we examined the adsorption modes and energies for 1-propyl, 2-propyl, propylidene, propylidyne, 1-propenyl, 2-propenyl, propenylidene and propynyl at a surface coverage of 0.25 ML corresponding to a 2x2 unit cell. We determined the relative stabilities

and the most favourable adsorption sites for all the above species. For the C_3H_x (x=3–7) fragments, there appears to be a general trend that Pt(111) prefers sp^3 bound intermediates. The relative stabilities of 1-propyl, 2-propyl, propylidene, propylidyne, 1-propenyl, 2-propenyl, propyne, propenylidene and propynyl are –69, –56, –68, –145, –93, –89, –104, –123 and –40 $kJmol^{-1}$, respectively. Propylidyne is the most stable surface species on Pt(111) well in line with the experimental evidence.

We computed the reaction energies for 18 elementary steps that may potentially be involved in the propylene-to-propylidyne transformation. Our calculations clearly indicate that the dehydrogenation of propylene to propylidyne is thermodynamically favourable. Besides, the formation of propynyl is energetically unfavourable and we concluded that is species may not be involved in the direct reaction of dehydrogenation.

Moreover, we simulated the vibrational spectra for propylene, propylidyne and the possible reaction intermediates. Our results for propylene and proplidyne are quite consistent with the experimental data. Unfortunately, the experimental data available for the reaction intermediate is not enough for an unequivocal identification. Our best guesses are: propylidene and 1-propenyl.

We also studied the surface structure and stability of a propylene-sulphate complex. We showed that the formation of this intermediate is energetically favoured and provided a theoretical support to the experimental observations. We proposed the surface structure for this alkyl-sulphate complex and demonstrated that the interaction of propylene with sulphate species activates the hydrocarbon molecule up to a large extent. Moreover, we showed that the simulated IR spectrum of the adsorbed alkyl-sulphate can be very useful to the identification of this surface species. The peaks at 1078 and 1047 cm^{-1} and the splitting of the SO_4 group frequencies of the sulphate unit are the fingerprint of this intermediate.

4.5 References and Notes

[1] F. Zaera, *Chem. Rev.* 95 (1995) 2651.
[2] P.C. Stair, G.A. Somorjai, *Chem. Phys. Lett.* 41 (1976) 391.
[3] L.L. Kesmodel, L.H. Dubois, G.A. Somorjai, *Chem. Phys. Lett.* 56 (1978) 267.
[4] R.J. Koestner, J.C. Frost, P.C. Stair, M.A. van Hove, G.A. Somorjai, *Surf. Sci.* 116 (1982) 85.
[5] L.L. Kesmodel, L.H. Dubois, G.A. Somorjai, *J.Chem. Phys.* 70 (1979) 2180.
[6] X.-Y. Zhou, X.-Y. Zhu, J.M. White, *Surf. Sci.* 193 (1988) 387.
[7] D.B. Kang, A.B. Anderson, *Surf. Sci.* 155 (1985) 639.
[8] A.B. Anderson, S.J. Choe, *J. Phys. Chem.* 93 (1989) 6145.
[9] E.A. Carter, B.E. Koel, *Surf. Sci.* 226 (1990) 339.
[10] D. Godbey, F. Zaera, R. Yeates, G. A. Somorjai, *Surf. Sci.* 167 (1986) 150.
[11] F. Zaera, *J. Am. Chem. Soc.* 111 (1989) 4240.
[12] M. Salmerón, G. A. Somorjai, *J. Phys. Chem.* 86 (1982) 341.
[13] N. R. Avery, N. Sheppard, *Proc. R. Soc. Lond. A* 405 (1986) 1.
[14] A. Cassuto, M. Mane, G. Tourillon, P. Parent, J. Jupille, *Surf. Sci.* 287/288 (1993) 460.
[15] A. B. Anderson, D.B. Kang, Y. Kim, *J. Am. Chem. Soc.* 106 (1984) 6597.
[16] Y.-L. Tsai, C. Xu, B.E. Koel, *Surf. Sci.* 385 (1997) 37.
[17] F. Zaera, D. Chrysostomou, *Surf. Sci.* 457 (2000) 71; ibid. 457(2000)89.

[18] H. Steininger, H. Ibach, S. Lewald, *Surf. Sci.* 117 (1982) 685.
[19] C. E. Anson, N. Sheppard, B. R. Bender, J.R. Norton, *J. Am. Chem. Soc.* 121 (1999) 529.
[20] K.M. Ogle, J.R. Creighton, S. Akhter, J.M. White, *Surf. Sci.* 169 (1986) 246.
[21] S. Brunet, D. Mey, G. Perot, C. Bouchy, F. Diehl, *Appl. Catal. A General* 278 (2005) 143.
[22] K. Wilson, C. Hardacre, R.M. Lambert, *J. Phys. Chem.* 99 (1995) 13755.
[23] K. Wilson, A.F. Lee, C. Hardacre, R.M. Lambert, *J. Phys. Chem. B* 102 (1998) 1736.
[24] A.F. Lee, K. Wilson, R.M. Lambert, C.P. Hubbard, R.G. Hurley, R.W. McCabe, H.S. Ghandi, *J. Catal.* 184 (1999) 491.
[25] A.F. Lee, K. Wilson, A. Goldoni, R. Larciprete, S. Lizzit, *Surf. Sci.* 513 (2002) 140.
[26] A.F. Lee, K. Wilson, A. Goldoni, R. Larciprete, S. Lizzit, *Catal. Lett.* 78 (2002) 379.
[27] B. Hammer, L. B. Hansen, J. Nørskov, *Phys. Rev. B* 59 (1999) 7413.
[28] F. Delbecq, P. Sautet, *J. Catal*. 211 (2002) 398.
[29] Angle between the C^1–C^2 bond and the C^1H_2 plane.
[30] Q. Ge, D. A. King, *J. Chem. Phys.* 110 (1999) 4699.
[31] G. W. Watson, R. P. K. Wells, D. J. Willock, G. J. Hutchings, *J. Phys. Chem. B* 104 (2000) 6439.
[32] A. Valcárcel, A. Clotet, J.M. Ricart, F. Delbecq, P. Sautet, *Surf. Sci.* 549 (2004) 121.
[33] Q. Ge, D.A. King, *J. Chem. Phys.* 110 (1999) 4699.
[34] M. J. Frisch et al., Gaussian 98 revision A6, Gaussian Inc., Pittsburgh, PA, 1998
[35] A.D. Becke, *J. Chem. Phys.* 98 (1993) 5648.
[36] D. Curulla, A. Clotet, J.M. Ricart and F. Illas, *J. Phys. Chem. B* 103 (1999) 5246.
[37] P. Hay and W. R. Wadt, *J. Chem. Phys.* 82 (1985) 299.
[38] S. Zurita, F. Illas, J. C. Barthelat, J. Rubio, *J. Chem. Phys*. 104 (1996) 8500.
[39] S. F. Boys, F. Bernardi, *Mol. Phys.* 19 (1970) 553.
[40] R. W. G. Wyckoff, *Crystal Structures*, 2nd ed., vol. 1, Interscience Publishers, New York (1965).
[41] R. Hoffmann, *Solids and surfaces*, VCH, New York (1988).
[42] E. Schustorovich, R.C. Baetzold, *Science* 227 (1985) 876.
[43] R. A. van Santen, *Cat. Lett.* 16 (1992) 59.
[44] M. Neurock, R. A. van Santen, *J. Phys. Chem. B* 104 (2000) 11127.
[45] S. G. Podkolzin, R. Alcalà, J.A. Dumesic, *J. Molec. Catal. A* 218 (2004) 217.
[46] These modes are strongly affected by the anharmonicity.
[47] M.A. Chesters, C. de la Cruz, P. Gadner, E. M. McCash, P. Pudney, G. Shahid, N. Sheppard, *J. Chem. Soc. Faraday Trans.* 86 (1990) 2757.
[48] X. Lin, W.F. Schneider, B.L. Trout, *J. Phys. Chem. B* 108 (2004) 250.
[49] K. Wilson, C. Hadacre, C.J. Baddeley, J. Lüdecke, D.P. Woodruff, R.M. Lambert, *Surf. Sci.* 372 (1997) 279.